Journal of Applied Polymer Science

5-Fluorouracil encapsulated magnetic nanohydrogels for drug-delivery applications

Tippabattini Jayaramudu,[1,2,3] Gownolla Malegowd Raghavendra,[2,4] Kokkarachedu Varaprasad,[5] Konduru Mohana Raju,[2] Emmanuel Rotimi Sadiku,[3] Jaehwan Kim[1]

[1]Center for Nano Cellulose Future Composites, Department of Mechanical Engineering, Inha University, 253 Yonghyun-Dong, Nam-Ku, Incheon 402-751, South Korea

[2]Synthetic Polymer Laboratory, Department of Polymer Science and Technology, Sri Krishnadevaraya University, Anantapur 515003, India

[3]Department of Polymer Technology, Tshwane University of Technology, Council for Scientific and Industrial Research Campus, Lynwood Ridge, Pretoria, South Africa

[4]Department of Packaging, Yonsei University, 1 Yonseidae-Gil, Wonju, Gangwon-Do 220-710, Korea

[5]Centro de Investigación de Polímeros Avanzados (CIPA), Avenida Collao 1202, Edificio de Laboratorio CIPA, Concepción, Chile

Correspondence to: T. Jayaramudu (E-mail: mr.jayaramudu@gmail.com) and K. Varaprasad (E-mail: varmaindian@gmail.com or prasad@cipachile.cl)

ABSTRACT: For the first time, green-tea (GT)-based magnetic nanohydrogels were developed for drug-delivery purposes. The hydrogel matrices were fabricated via the *in situ* polymerization of acrylamide with GT molecules. Magnetic nanoparticles were synthesized by the reduction of the 1:2 molar ratio mixture of ferrous sulfate heptahydrate and ferric chloride hexahydrate with an ammonia solution. A chemotherapeutic drug, 5-fluorouracil, was chosen as a model drug, and its releasing profiles in the presence and absence of the external magnetic field were evaluated at a pH of 7.4. We observed that in the presence of the applied magnetic field, these magnetic nanohydrogels released 2.86% more drug than in the absence of a magnetic field. The magnetic nanohydrogels were characterized by X-ray diffraction, Fourier transform infrared spectroscopy, scanning electron microscopy, vibrating sample magnetometry, and transmission electron microscopy. © 2016 Wiley Periodicals, Inc. J. Appl. Polym. Sci. **2016**, *133*, 43921.

KEYWORDS: biocompatibility; biomedical applications; drug-delivery systems; gels; hydrophilic polymers

Received 27 January 2016; accepted 8 May 2016

DOI: 10.1002/app.43921

INTRODUCTION

Magnetic nanoparticles (MNPs), in particular, show a significant adsorption capacity because of their higher surface area and better active sites for interaction with drug molecules.[1–4] Because of this, the application of magnetic nanohydrogels in the field of drug delivery has become a very interesting area of research. In general, magnetic nanohydrogels are hydrophilic polymeric network structures, where the MNPs are stabilized with crosslinked network structures of the hydrogel; this can expand their volume in aqueous medium and release the MNPs' absorbed drug at the site location.[5] On the basis of these significant behaviors, magnetic nanohydrogels have been widely used in several applications, such as cancer drug delivery, hyperthermia, magnetic separation, MRI contrast agents, tissue engineering, and thermal applications.[5–8]

In recent years, natural magnetic nanohydrogels have been developed for biomedical applications because of their low cost, nontoxicity, ecofriendliness, and potential degradability.[5,9,10] From natural materials, we chose green tea (GT) as the point of focus of our study because of its significant properties and biomedical values.

GT is a phytochemical product produced from unfermented tea leaves (*Camellia sinensis*).[11] It is an ecofriendly, low-cost, naturally existing material, and it is the most widely consumed beverage. Polyphenols are the main constituents present in GT, and they have been demonstrated[11,12] to possess significant properties, including antioxidant, anticarcinogenic, and anti-inflammatory properties. Furthermore, the major constituent of the polyphenol component of GT is epigallocatechin-3-gallate, which is a pharmacologically active compound.[13–16]

Additional Supporting Information may be found in the online version of this article.

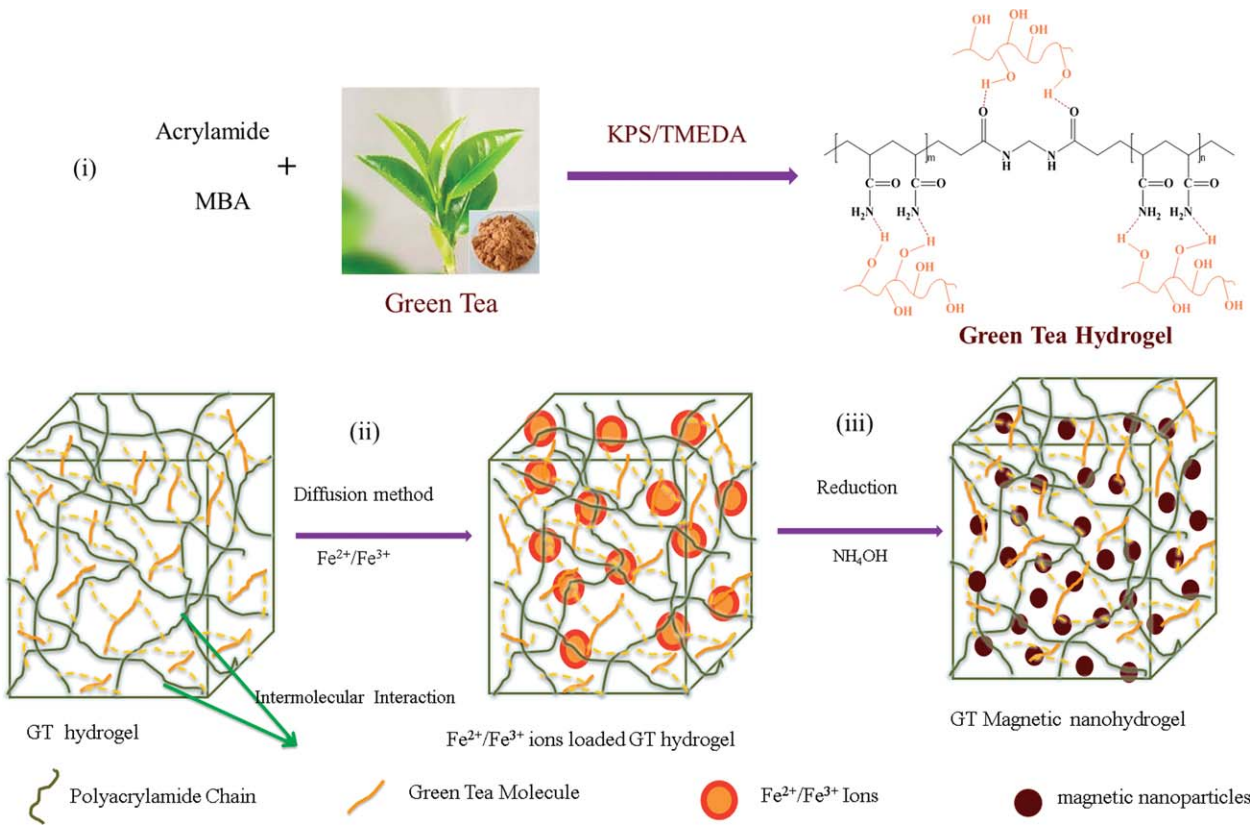

Figure 1. Schematic diagram for the formation of the GT and magnetic nanohydrogels. [Color figure can be viewed in the online issue, which is available at wileyonlinelibrary.com.]

It has been demonstrated that GT can act as a reducing and capping agent for metal nanoparticles.[17,18] Because of this significant nature, GT has become a close and highly relevant material in the field of nanotechnology. Wang *et al.*[19] synthesized iron nanoparticles with GT-based materials. Shahwan *et al.*[17] reported on functional iron-based nanoparticles synthesized with tea extract as a catalyst. Some researchers have prepared antimicrobial silver and gold nanoparticles with tea leaf extracts.[18,20]

Although GT has numerous features that are closely associated with nanotechnology and biomedical applications, the integration of GT into hydrogel systems in a combination of nanotechnologies is rather new. Hence, we carried out this study to fabricate GT-based magnetic nanohydrogels via a diffusion technique, where the necessary MNPs were synthesized by the reduction of a 1:2 molar ratio of ferrous sulfate heptahydrate ($FeSO_4{\cdot}7H_2O$) and ferric chloride hexahydrate ($FeCl_3{\cdot}6H_2O$) with an ammonia solution. Structural and morphological studies of the developed hydrogels were carried out with Fourier transform infrared (FTIR) spectroscopy and X-ray diffraction (XRD), and the magnetic properties of the MNPs formed were confirmed with vibrating sample magnetometry (VSM). The thermal stability, surface morphology, and content and distribution of MNPs in the hydrogels were determined by thermogravimetric analysis (TGA), differential scanning calorimetry (DSC), scanning electron microscopy (SEM)/energy-dispersive spectroscopy (EDS), and transmission electron microscopy (TEM). Furthermore, 5-fluorouracil (5-Fu), a pyrimidine analog that is widely used in cancer treatments, such as breast, stomach, pancreas, ovaries, colon, and bladder cancer treatments, was chosen as a model drug.[21–23] The drug-releasing patterns, which were evaluated in phosphate buffer at pH 7.4, both in the presence and absence of the external magnetic field, are summarized later.

EXPERIMENTAL

Materials

Acrylamide (AM), *N,N′*-methylenebisacrylamide (MBA), potassium persulfate (KPS), and *N,N,N′,N′*-tetramethylethilenediamine (TMEDA), Ammonium hydroxide (NH_4OH) were purchased from S.D. Fine Chemicals (Mumbai, India). GT extract (80% polyphenols) was obtained as a gift sample from Natural Remedies Private, Ltd. (Bangalore, India). 5-Fluorouracil (5-Fu) was purchased from Aldrich Chemicals. Ferrous sulfate heptahydrate ($FeSO_4.7H_2O$) and Ferric chloride hexahydrate ($FeCl_3{\cdot}6H_2O$) were purchased from Merck (Mumbai, India). All chemicals were used without further purification. Double-distilled water was used throughout the experiments.

Synthesis of the Magnetic Nanohydrogels

The preparation of the magnetic nanohydrogels consisted of three steps, and these are shown schematically in Figure 1: (1) the preparation of GT hydrogels via *in situ* free-radical polymerization, (2) the loading of iron (Fe^{2+}/Fe^{3+}) ions into the

Table I. Feed Compositions of the GT Hydrogels Prepared at Room Temperature with Stirring at 100 rpm for 30 min

Hydrogel code	AM (*M*)	GT (g)	MBA (*M*)	KPS (*M*)	TMEDA (*M*)
GT_0	14.084	—	0.648	1.851	0.8620
GT_1	14.084	0.0025	0.648	1.851	0.8620
GT_2	14.084	0.005	0.648	1.851	0.8620
GT_3	14.084	0.0075	0.648	1.851	0.8620
GT_4	14.084	0.01	0.648	1.851	0.8620

hydrogels via a swelling method, and (3) the development of magnetic nanohydrogels via a chemical process (where the reduction of Fe^{2+}/Fe^{3+} ions occurred via ammonia solution, which led to the formation of MNPs throughout the hydrogel network).

Preparation of the GT Hydrogels

Typically, 14.08 mmol of AM and between 0.0025–0.01 g of GT were dissolved in 2 mL of double-distilled water under the stirring (100 rpm) condition at room temperature for 30 min. To this mixture solution, 0.648 mmol of MBA and 1.851/0.862 mmol of KPS/TMEDA (initiating pair) were added to initiate the polymerization process, which led to the formation of hydrogels at room temperature within 30 min. The formed hydrogel matrix was carefully transferred to a 500 mL beaker containing 250 mL of distilled water, and the distilled water was repeatedly changed (every 8 h) for 24 h to remove the unreacted products, such as monomer, crosslinker, initiator, and soluble polymers.[24] The obtained GT hydrogels were allowed to dry at ambient temperature for 24 h. Similarly, other hydrogel formulations were fabricated with the previous procedure. The feed composition of the fabricated hydrogels is shown in Table I.

Entrapment of Fe^{2+}/Fe^{3+} Ions in the Hydrogel Network via Swelling

The hydrogels synthesized method were placed individually in 50 mL of double-distilled water and allowed to reach equilibrium swelling over a period of 24 h. The swollen hydrogels were transferred to another beaker containing 50 mL of solution, which consisted of a 1:2 molar ratio of $FeSO_4{\cdot}7H_2O$ and $FeCl_3{\cdot}6H_2O$ (Fe^{2+}/Fe^{3+} solutions), and allowed to stand overnight at room temperature to entrap the iron ions throughout the hydrogel networks.

Conversion of Fe^{2+}/Fe^{3+}Ions into MNPs in the GT Hydrogel Network

The Fe-ion-entrapped hydrogels were removed from the Fe^{2+}/Fe^{3+} solutions, washed with double-distilled water to remove Fe ions on the surface of the hydrogel, placed in a 50 mL of a 0.5-*M* ammonia solution, and left overnight. In this step, the Fe ions were converted into MNPs. The resulting nanohydrogels appeared to be dark brown. They were removed, washed with double-distilled water, and allowed to dry at ambient temperature for 48 h. The GT magnetic nanohydrogels were used for further studies.

Characterization of the Magnetic Hydrogels

FTIR Spectroscopy. The pure GT, GT hydrogels, and their magnetic nanohydrogel network structures were studied with FTIR spectroscopy. The GT hydrogels and the MNP-embedded hydrogels were completely dried in an oven (Baheti Enterprises, Hyderabad, India) at 60 °C for 6 h before we carried out the FTIR experiments. Samples were examined between 500 and 4000 cm^{-1} on a Bruker IFS 66V FTIR spectrometer (Ettlingen, Germany) with the KBr disk method.

Thermal Analysis. Thermal analysis (TGA/DSC) of the samples was carried out with an SDT Q 600 DSC instrument (TA Instruments–Waters, LLC, Newcastle, DE) at a heating rate of 10 °C/min under a constant nitrogen flow (100 mL/min).

SEM/EDS Analysis. SEM/EDS analyses of the plain hydrogel and MNP-embedded hydrogels were performed with a JEOL JEM-7500F instrument (Tokyo, Japan) operated at an accelerating voltage of 15 kV. All of the hydrogels and magnetic nanohydrogels were iridium-coated before examination on a field emission scanning electron microscope.

XRD Analysis. The XRD method was used to identify the formation of MNPs in the hydrogels network. The measurements were carried out on dried and finely ground samples on a Rigaku diffractometer (Cu Kα radiation, $\lambda = 0.1546$ nm) at 15 kV and 50 mA.

TEM Analysis. TEM (JEM-1200EX, JEOL, Tokyo, Japan) was used for the morphological observation. The TEM sample was prepared by the dispersion of two to three drops of a finely ground magnetic nanohydrogel solution (1 mg/1 mL) on a 3-mm copper grid and dried at ambient temperature after the excess solution was removed with fine filter paper.

Magnetization Studies with VSM. Magnetization and hysteresis loops of the developed magnetic nanohydrogels were measured at room temperature with VSM (model 7300 VSM system, Lake Shore Cryotronic, Inc., Westerville, OH).

Water-Uptake Studies. Accurately weighed dry hydrogels were immersed in a 100 mL beaker containing double-distilled water for 48 h until the hydrogel reached equilibrium swelling at ambient temperature. The swollen hydrogels were treated with Fe^{2+}/Fe^{3+}, and subsequently, magnetic nanohydrogels were developed with an ammonia solution, as explained in the Experimental section. The water-uptake ratios of the developed hydrogels and their magnetic nanohydrogels were calculated with eq. (1):

$$\text{Water-uptake ratio} = (W_s - W_d)/W_d \quad (1)$$

where W_s and W_d are the weights of the swollen hydrogel (Fe^{2+}/Fe^{3+} or magnetic nanohydrogels in the swollen state) at equilibrium and the dry hydrogel, respectively. The provided data are the average values of three individual sample readings.

Table II. Encapsulation Efficiency and Cumulative Release for the GT_1 and GT_4 Hydrogels and the GT_1 and GT_4 Magnetic Nanohydrogels with and Without an External Magnetic Field

	GT-based hydrogels		GT-based magnetic nanohydrogels			
			Without magnetic field		With magnetic field	
	GT_1	GT_4	GT_1	GT_4	GT_1	GT_4
Encapsulation efficiency (%)	26.07	34.37	43.58	79.23	59.71	81.02
Cumulative release (%)	43.80	68.20	85.39	97.28	88.42	99.87
k	0.0046	0.0150	0.0129	0.0582	0.0380	0.0868
n	0.761	0.604	0.666	0.468	0.504	0.496

Data at pH 7.4 were applied, and the release kinetics parameters were assessed at 37 °C.

Drug-Loading Studies. A hydrophilic anticancer drug (5-Fu) was chosen as a model drug in a typical drug-loading process.[1,21] An amount of 100 mg of dry hydrogel and its magnetic nanohydrogels were allowed to attain equilibrium swelling in the drug solution (5 mg in 10 mL of distilled water) for 24 h at room temperature. Then, the swollen hydrogel was transferred to a disk and allowed to dry at ambient temperature for 24 h. The drug-loading efficiency of 5-Fu in the hydrogel and its magnetic nanohydrogels were determined at a maximum λ of 265 nm with an ELICO SL 164 ultraviolet–visible spectrophotometer (The Elico, Hyderabad, India). The percentage encapsulation efficiency was calculated with eq. (2). The results are depicted in Table II. Here, the percentage theoretical loading of 5-Fu was 5 mg:

$$\text{Encapsulation efficiency (\%)} = [\text{Actual loading (\%)} / \text{Theoretical loading (\%)}] \times 100 \quad (2)$$

***In Vitro* Drug-Release Studies.** An 80-kHz magnetic field was generated with an apparent current for release studies. We carried out *in vitro* drug-release studies of the 5-Fu drug by separately placing the 5-Fu-loaded GT hydrogels and 5-Fu-loaded GT magnetic nanohydrogels in a defined volume (25 mL) of pH 7.4 phosphate buffer medium. The drug-release kinetics were analyzed with the percentage of cumulative release data (M_t/M_0, where M_t is the amount of drug released at time t and M_0 is the initial amount of the drug loaded) as a function of time. We determined the amount of 5-Fu drug at different time intervals by recording the absorptions of the solutions at a maximum wavelength of 265 nm with an ultraviolet–visible spectrophotometer (model SL 164, Elico, Hyderabad, India).

RESULTS AND DISCUSSION

Hydrogels have excellent properties with superior absorption capacity in aqueous media. Therefore, when the hydrogels were immersed in the aqueous Fe^{2+}/Fe^{3+} ion solution, the ions easily penetrated into the hydrogel networks through absorption, and these ions were easily functionalized with the hydrophilic groups of the hydrogel networks by coordinating bonds.[25] When the ion-adsorbed hydrogels were immersed in an aqueous ammonia solution, a basic hydrolysis reaction occurred to form the MNPs.[26] Here, the hydrogel networks acted as stabilizing templates during the formation of the MNPs from the Fe^{2+}/Fe^{3+} ions. Equation (3) represents the formation of the MNPs:

$$Fe^{2+} + 2Fe^{3+} + 80H^- \rightarrow Fe_3O_4 + 4H_2O \quad (3)$$

FTIR Spectroscopy

The functional networks of the developed GT hydrogel and its magnetic nanohydrogels were investigated by FTIR analysis. Figure 2 shows the FTIR spectra of the pure GT, GT hydrogels, and their corresponding magnetic nanohydrogels. The characteristic bands in the FTIR spectrum of GT showed a broad absorption peak at 3261 cm^{-1}, which was assigned to the symmetric stretching vibrations of —OH, and the peaks at 820, 1030, 1138, 1230, 1322, 1450, 1517, and 1610 cm^{-1} indicated the presence of C—H alkenes, —C—O alcohols, C—OH alcohols, —OH aromatic, C—O alcohols, C—H alkenes, C=C aromatic ring, and C=C alkenes, respectively; this was consistent with data from previous reports.[27,28] The GT hydrogels (Figure 2) showed absorption peaks at 1641 and 1430 cm^{-1}; these were associated with the C=O stretching vibrations of AM and GT units, and the broad peak observed at 3291 cm^{-1} was due to the stretching vibrations of the NH_2 and OH functional groups in the hydrogel networks.[29] The magnetic nanohydrogels (Figure 2) did show all of the previous characteristic peaks, with a slight shift in wavelengths from 3291 to 3346 cm^{-1}; these corresponded to NH_2 and —OH functional groups. Those at 1658 and 1441 cm^{-1} were related to the C=O stretching vibrations of AM and GT, respectively, and a new sharp peak was observed at 603 cm^{-1} and was due to the stretching vibrations of the Fe—O of MNP. This confirmed the presence of iron oxide nanoparticles in the hydrogel matrix.[30] As a result, we concluded without a doubt that MNPs were present in GT hydrogels.

Thermal Analysis

The thermal stability and the formation of hydrogels and magnetic nanohydrogels were analyzed with TGA and DSC analysis. Figure 3 shows the DSC and TGA curves of the pure GT, GT_4 hydrogel (see see Table I for the compositions of the different hydrogel samples), and magnetic nanohydrogels. In the DSC thermogram, GT_4 hydrogel showed an exothermic peak at 230 °C due to the formation of intermolecular bonds between the GT (—OH) and polyacrylamide ($—CONH_2$) hydrogel network, whereas the magnetic nanohydrogels displayed a stronger

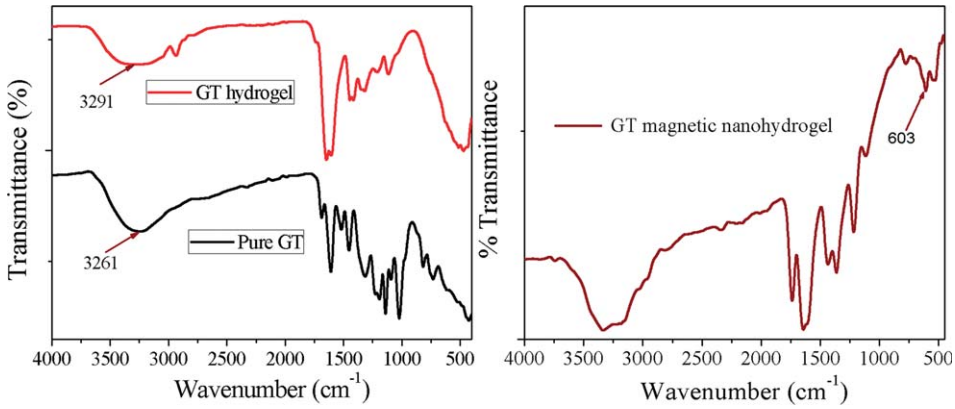

Figure 2. FTIR spectra of the pure GT, GT hydrogel, and GT_4 magnetic nanohydrogel. [Color figure can be viewed in the online issue, which is available at wileyonlinelibrary.com.]

exothermic peak at 240.5 °C when compared to the GT_4 hydrogel in the DSC [Figure 3(A)] studies. This was due to the incorporation of MNPs in the hydrogel network. A small endothermic peak was observed around 100 °C in all cases; that is, the pure GT, GT_4 hydrogel, and its magnetic nanohydrogels; this was due to the presence of moisture in the samples.

The percentage weight loss of the pure GT, GT_1 and GT_4 hydrogels, and their corresponding magnetic nanohydrogels was characterized by TGA to determine the weight loss at certain temperatures. Figure 3(B) shows the percentage decomposition of the hydrogel and its magnetic nanohydrogels. In the case of all of the developed hydrogels, initial weight loss occurred in the temperature range 50–100 °C because of the evaporation of moisture in the sample. A significant weight loss occurred around 193 °C, and this was due to the volatilization of organic species in the samples. However, from the TGA thermogram, the decomposition of GT_1 and GT_4 hydrogels occurred at 600 °C, with significant weight losses of 83.47 and 79.39% [Figure 3(B)], respectively. In the case of magnetic nanohydrogels, 60.11 and 55.54% weight losses occurred at 600 °C [Figure 3(B)]. Moreover, according to the TGA results, the magnetic nanohydrogels showed a higher thermal stability than the GT hydrogel.

SEM/EDS Analyses

The surface morphology of the GT_4 and magnetic nanohydrogels were investigated with SEM. Figure 4(A,B) shows the SEM micrographs of the GT_4 and magnetic nanohydrogels. Figure 4(A) shows clearly a rough surface for the GT_4 hydrogel, whereas the magnetic nanohydrogels exhibited a distributed pattern corresponding to Fe_3O_4. Furthermore, the particles did not ooze out, rather they were entrapped within the matrix; this indicated a strong interaction between the GT hydrogel and the MNPs.

To determine the identity of the MNP elements in the hydrogel, EDS analysis was carried out. The EDS spectra of the GT hydrogels and magnetic nanohydrogels are presented in Figure 4(C,D). The EDS spectrum for the nonmagnetic hydrogel did not show the characteristic peak of Fe [Figure 4(C)], whereas the magnetic nanohydrogels showed Fe in addition to O [Figure 4(D)]. It was clear that the magnetic nanohydrogels consisted of Fe and O; this further confirmed the appearance of MNPs in the hydrogel network.

XRD analysis

Figure 5(A) shows the XRD pattern of the pure GT, GT_4 hydrogel, and their magnetic nanohydrogels. In Figure 5(A), the

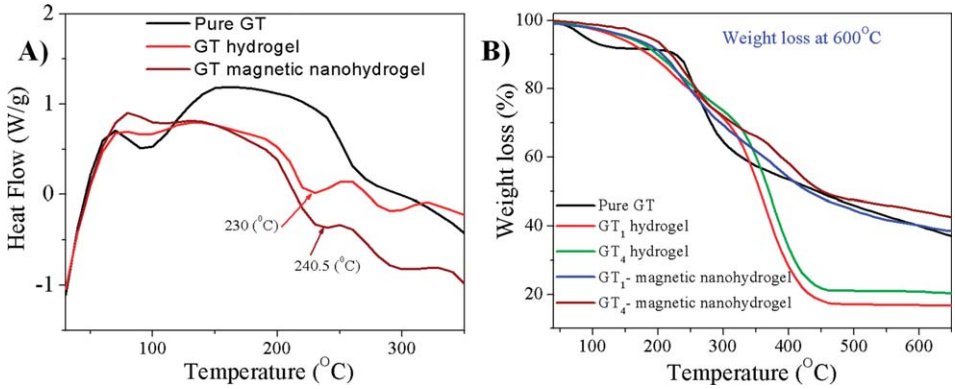

Figure 3. (A) DSC thermograms of the pure GT, GT_4 hydrogel, and GT_4 magnetic nanohydrogel and (B) TGA curves of the pure GT, GT_1 and GT_4 hydrogels, and GT_1 and GT_4 magnetic nanohydrogels. [Color figure can be viewed in the online issue, which is available at wileyonlinelibrary.com.]

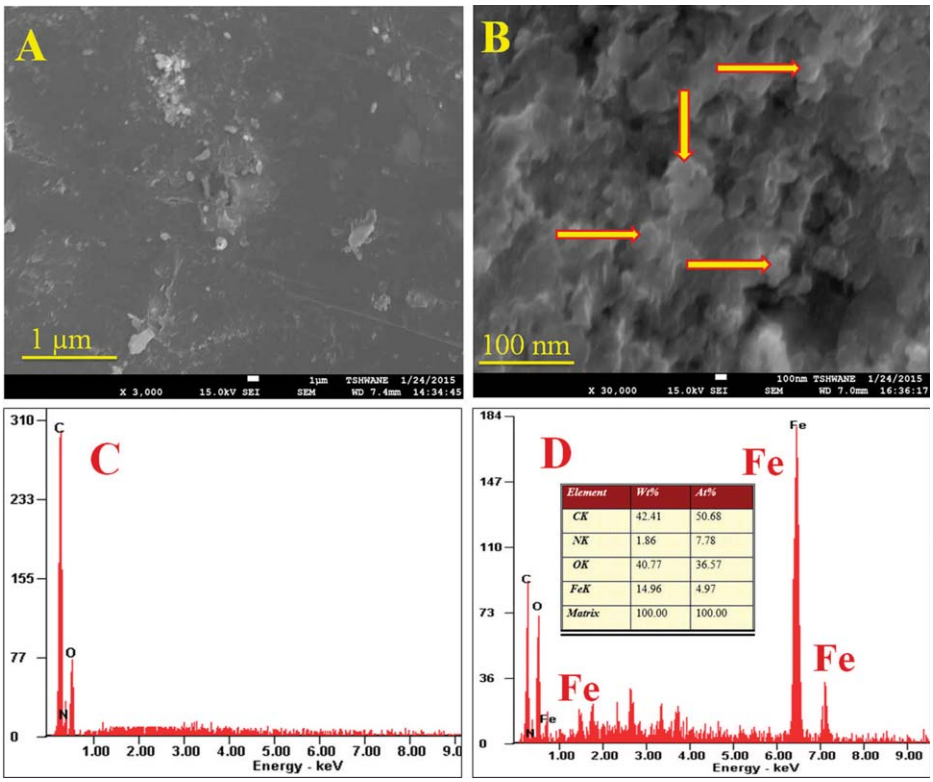

Figure 4. SEM images of the (A) GT_4 hydrogel and (B) GT_4 magnetic nanohydrogel and EDS images of the (C) GT_4 hydrogel and (D) GT_4 magnetic nanohydrogel. [Color figure can be viewed in the online issue, which is available at wileyonlinelibrary.com.]

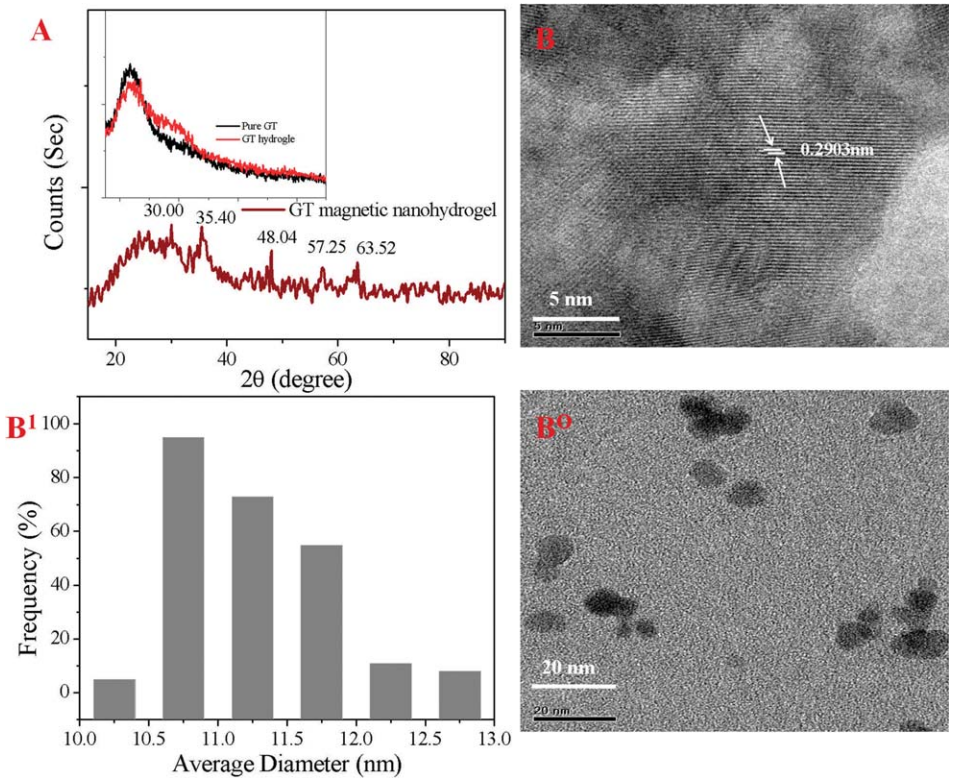

Figure 5. XRD patterns of the (A) pure GT, GT_4 hydrogel, and GT_4 magnetic nanohydrogel; (B) TEM image of the magnetic nanohydrogel; (B^0) low-magnification image; and (B^1) MNP sizes calculated from the TEM images with ImageJ software. [Color figure can be viewed in the online issue, which is available at wileyonlinelibrary.com.]

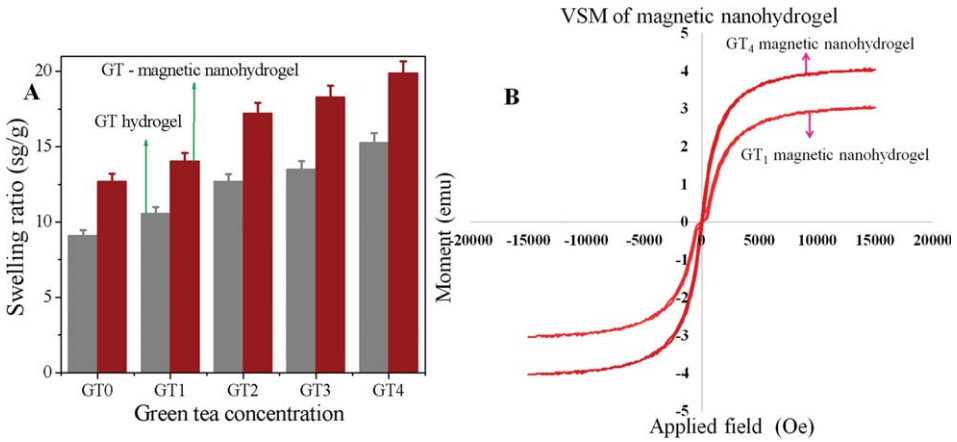

Figure 6. (A) Water uptake of the GT hydrogel and GT magnetic nanohydrogel and (B) magnetization saturation curves of the GT_1 and GT_4 magnetic nanohydrogels. [Color figure can be viewed in the online issue, which is available at wileyonlinelibrary.com.]

magnetic nanohydrogels showed diffraction peaks at 2θ values of 30.00° (220), 35.40° (311), 48.04° (400), 57.25° (511), and 63.52° (440).[31–33] The peaks were identified with WinXPow software, and they coincided with the data of cubic magnetic (JCPDS card no. 19-0629). Generally, the magnetite (magnetic) and maghemite peaks are observed at 35.423° (JCPDS 19-629) and 35.631° (JCPDS 39-1346), respectively.[34,35] Hence, these results were in good agreement with Bajapai *et al.*'s report.[36] Therefore, we confirmed the magnetic phase of the hydrogel, which stabilized the MNPs within their network.[37] However, in the cases of the pure GT and GT_4 hydrogel, these diffraction peaks were absent. However, regardless of their nature, all of the samples exhibited a common peak at a 2θ of 23.45°, which corresponded to their amorphous components.

TEM Analysis

The MNP size and shape were determined with TEM. Figure 5(B) shows the TEM image of MNPs that was extracted from the magnetic nanohydrogels (1 mg of magnetic nanohydrogels/1 mL of distilled water). It explains the fact that the MNPs were spherical in shape and were highly agglomerated with a diameter of approximately 10 ± 2 nm. At higher magnification, the interplanar *d*-spacing of 0.2903 nm is clearly visible in Figure 5(B). These studies explain the fact that the MNPs were highly capped and stabilized by GT in the hydrogels network;[38] this will enhance their applicability in drug delivery.

Water-Uptake Studies

The water-uptake capacity plays a vital role in inorganic hydrogels for advanced drug-delivery studies. The swelling behavior of the GT hydrogel and magnetic nanohydrogels are shown in Figure 6(A). In this investigation, we noticed that the rate of water-uptake was influenced by the GT concentrations. An increase in the GT concentration in the hydrogels increased the water-uptake capacity; this was due to the hydrophilic nature of the GT. We also observed that there was an increase in the water-uptake capacity in the magnetic nanohydrogels. The overall order of the water-uptake capacity followed in this manner: Magnetic nanohydrogels > GT hydrogel. When the hydrogels were treated with Fe^{2+}/Fe^{3+} ions, the ions were diffused and physically entrapped within the three-dimensional network of the hydrogel matrix, and when the Fe^{2+}/Fe^{3+} ions embedded hydrogels were treated with ammonia, MNPs were formed throughout the hydrogel structure, and the MNPs formed were capped and stabilized with the GT hydrogel network.[38,39] During the formation of MNPs in the hydrogels, the free space within the hydrogel networks was slightly increased; this allowed the uptake of more water molecules.[40] Therefore, a higher water-uptake capacity was observed in the magnetic nanohydrogels than in the GT hydrogels.

Magnetization Studies with VSM

The magnetic properties of the magnetic nanohydrogels were studied with VSM. The magnetization measurement obtained at room temperature for the magnetic nanohydrogels with the VSM technique is shown Figure 6(B). The saturation

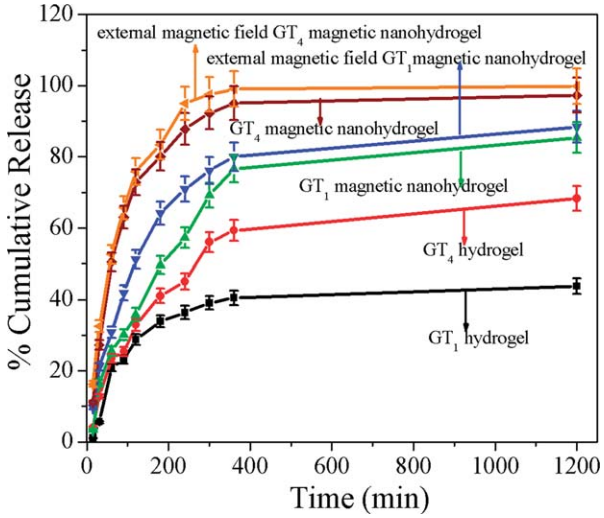

Figure 7. 5-Fu release profiles of GT_1 and GT_4 and their corresponding magnetic nanohydrogels in the presence and absence of an external magnetic field. [Color figure can be viewed in the online issue, which is available at wileyonlinelibrary.com.]

magnetization[40] was calculated from the plot of magnetic moment (M) as a function of magnetic field (H). No coercivity or remanence was observed in the magnetic loop, and this suggested superparamagnetic properties of the MNPs. The saturated magnetization values of the GT_1 and GT_4 magnetic nanohydrogels were 3.032 and 4.03 emu/g, respectively; these values were less than that of the pure MNPs because of the nonmagnetic behavior of the GT hydrogel matrix that surrounded the MNPs. The saturation magnetization of the magnetic nanohydrogels mainly depended on the volume fraction (anisotropy) of the MNPs that were present in the hydrogel network.[41] Furthermore, from of this study, we concluded from the saturated magnetization values that the GT_4 magnetic nanohydrogels contained more MNPs than the GT_1 magnetic nanohydrogels. We noted that the magnetic nanohydrogels acquired enough saturation magnetization that they would be feasible for most biomedical applications,[42] and they could provide an easy and capable system for carrying drugs to targeted locations. The magnetic content in the magnetic nanohydrogels was further determined by the TGA experiments [Figure 3(B)].

In Vitro Drug-Release Studies

It was reported that the drug-loading capacity is directly proportional to the swelling capacity.[1,23,43] The same was observed in this study. We observed that a higher amount of 5-Fu was released in GT_4 than in GT_1. This was in accordance with the swelling studies [Figure 6(A)]. Furthermore, we noticed that the magnetic GT_1 and GT_4 nanohydrogels released more 5-Fu drug when compared with the pure GT_4 and GT_1 hydrogels. This was the result of the greater availability of free space between the hydrogel networks, and therefore, more 5-Fu molecules were absorbed and bonded over the surface of the MNPs.[44] In the case where an external magnetic field was present, the release of 5-Fu was improved in the magnetic nanohydrogels (Figure 7). This was due to interactions between the external magnetic field and the magnetic particles (MNPs); the MNPs tended to align themselves in the same direction of the applied magnetic field; as a result, mechanical deformation of the hydrogel occurred, and this resulted in the squeezing out of the drug when compared with the absence of external magnetic field. Thus, an improved release of 5-Fu was observed under the magnetic field. During drug release, agglomeration is generally expected because of magnetism. However, the generated MNPs in the hydrogel system were at the nanolevel and acquired a precisely small magnetic momentum. Furthermore, these MNPs were sparsely distributed and, in turn, stabilized by GT hydrogel network, which provided effective shielding for responding to the low-intensity nanomagnetic domain generated by the surrounding MNPs. This shielding effectively passivated the agglomeration among the MNPs. Furthermore, as the external magnetic field was quantitatively higher in magnitude than the individual MNPs, the effect of the external magnetic field was more pronounced. Hence, it positively impacted the release of the drug. Similar types of results have been reported in the literature.[45–47] The 5-Fu release profile has been shown to have a 2.86% increase in drug release. This was due to the application of an external magnetic field. Upon the application of an external magnetic field, the alignment of MNPs within the hydrogel network took place; this caused the hydrogel network to expand. The resulting mechanical deformation of the gel squeezed the drug out and, thereby, allowed more 5-Fu molecules to be released into the medium.[48] The results indicate that GT_1 and GT_4 and their corresponding magnetic nanohydrogels without and with the application of an external magnetic field displayed cumulative releases of 43.80, 68.20, 85.39, 97.01, 88.42, and 99.87%, respectively, in 20 h.

Drug-Release Kinetics

The *in vitro* 5-Fu drug-release profiles of the GT hydrogel and magnetic nanohydrogels with and without the application of an external magnetic field are shown in Figure 7. The drug-release data were calculated as follows:

$$M_t/M_\infty = kt^n \quad (4)$$

where M_t/M_∞ is the fractional release of the drug at time t, k is a constant incorporating the structural and geometric characteristics of the release device, and n is the release exponent indicating the mechanism of release. With the least squares procedure, the n and k values of the GT hydrogel and magnetic nanohydrogels with or without the application of an external magnetic field were calculated and are shown in Table II. The n value played an important role in the mechanism of drug carrying, and in general, the n value is between 0.5 to 1.0. When $n = 0.5$, the release is Fickian diffusion. When $n = 1.0$, the release is zero-order kinetics; that is, the release is constant with time. Between these values ($0.5 < n < 1.0$), the release is described as anomalous (non-Fickian diffusion). When n is close to 1.0, the release pattern is close to a steady-state phenomenon.[49] However, the n and k values depend on the type of hydrogel system. The values of n for the GT_1 and GT_4 magnetic nanohydrogels were found to be Fickian, that is, 0.504 (GT_1) and 0.496 (GT_4), in the presence of the external magnetic field.[50] However, in the absence of the external magnetic field, GT_1 and GT_4 were found to show non-Fickian release: 0.666 (GT_1) and 0.468 (GT_4). Conversely, the blank hydrogels of GT_1 and GT_4 showed n values of 0.761 and 0.604, respectively; this indicated non-Fickian transport.

CONCLUSIONS

The presence of GT in the hydrogels was found improve the hydrogels' water-uptake ability and stabilized the MNPs in the hydrogel networks. Hydrogels containing MNPs were found to exhibit higher swelling ratios than the blank hydrogel. The successful development of the MNPs in the hydrogels was confirmed by FTIR spectroscopy, which showed the characteristic absorption peak for Fe—O at 603 cm^{-1}. This was further confirmed by XRD and SEM, and the nanoparticles' average size was approximately 10 ± 2 nm, as observed via TEM. The magnetic properties of the developed magnetic nanohydrogels was studied with VSM. The drug-release profile suggested that the rate of drug release could be increased through an increase in the amount of GT in the hydrogels. The drug-release profiles of the magnetic nanohydrogels were studied in the absence and presence of an external magnetic field. The release kinetics of 5-Fu from the magnetic nanohydrogels was found to differ with the application of an external magnetic field. At pH 7.4, the

application of the external magnetic field of the drug-release profile was found to show Fickian diffusion for both the GT_1 and GT_4 magnetic nanohydrogels with n values of 0.504 and 0.496, respectively; this suggested that the developed magnetic nanohydrogels exhibited superparamagnetic and biocompatible properties, and therefore, these are suitable potential candidates for biomedical (drug-delivery) applications.

ACKNOWLEDGMENTS

This research was supported by the National Research Foundation of Korea (contract grant number NRF-2015R1A3A2066301) and the author Kokkarachedu Varaprasad wishes to acknowledge the Programa de Atracción e Inserciůn de Capital Humano Avanzado (PAI) Proyecto No. 781302011, CONICYT, Chile and the CIPA, CONICYT Regional PRFC0002.

REFERENCES

1. Satarkar, N. S.; Hilt, J. Z. *J. Controlled Release* **2008**, *130*, 246.
2. Namdeo, M.; Saxena, S.; Tankhiwale, R.; Bajpai, M.; Mohan, Y.; Bajpai, S. *J. Nanosci. Nanotechnol.* **2008**, *8*, 3247.
3. Gaihre, B.; Khil, M. S.; Lee, D. R.; Kim, H. Y. *Int. J. Pharm.* **2009**, *365*, 180.
4. Barbucci, R.; Pasqui, D.; Giani, G.; De Cagna, M.; Fini, M.; Giardino, R.; Atrei, A. *Soft Matter* **2011**, *7*, 5558.
5. Reddy, N. N.; Varaprasad, K.; Ravindra, S.; Reddy, G. S.; Reddy, K.; Reddy, K. M.; Raju, K. M. *Colloids Surf. A* **2011**, *385*, 20.
6. Kim, J. I.; Chun, C.; Kim, B.; Hong, J. M.; Cho, J.-K.; Lee, S. H.; Song, S.-C. *Biomaterials* **2012**, *33*, 218.
7. Meenach, S. A.; Hilt, J. Z.; Anderson, K. W. *Acta Biomater.* **2010**, *6*, 1039.
8. Jaiswal, M. K.; Gogoi, M.; Dev Sarma, H.; Banerjee, R.; Bahadur, D. *Biomater. Sci.* **2014**, *2*, 370.
9. Helminger, M.; Wu, B.; Kollmann, T.; Benke, D.; Schwahn, D.; Pipich, V.; Faivre, D.; Zahn, D.; Cölfen, H. *Adv. Funct. Mater.* **2014**, *24*, 3187.
10. Reddy, N. N.; Mohan, Y. M.; Varaprasad, K.; Ravindra, S.; Joy, P. A.; Raju, K. M. *J. Appl. Polym. Sci.* **2011**, *122*, 1364.
11. Namal Senanayake, S. P. J. *J. Funct. Foods* **2013**, *5*, 1529.
12. Manea, A.-M.; Vasile, B. S.; Meghea, A. C. R. *Chim* **2014**, *17*, 331.
13. Yang, C. S.; Li, G.; Yang, Z.; Guan, F.; Chen, A.; Ju, J. *Cancer Lett.* **2013**, *334*, 79.
14. Sakakibara, H.; Honda, Y.; Nakagawa, S.; Ashida, H.; Kanazawa, K. *J. Agric. Food Chem.* **2003**, *51*, 571.
15. Yoshizawa, S.; Horiuchi, T.; Fujiki, H.; Yoshida, T.; Okuda, T.; Sugimura, T. *Phytother. Res.* **1987**, *1*, 44.
16. Jankun, J.; Selman, S. H.; Swiercz, R.; Skrzypczak-Jankun, E. *Nature* **1997**, *387*, 561.
17. Shahwan, T.; Abu Sirriah, S.; Nairat, M.; Boyacı, E.; Eroğlu, A. E.; Scott, T. B.; Hallam, K. R. *Chem. Eng. J.* **2011**, *172*, 258.
18. Sharma, R. K.; Gulati, S.; Mehta, S. *J. Chem. Educ.* **2012**, *89*, 1316.
19. Wang, T.; Lin, J.; Chen, Z.; Megharaj, M.; Naidu, R. *J. Cleaner Prod.* **2014**, *83*, 413.
20. Sun, Q.; Cai, X.; Li, J.; Zheng, M.; Chen, Z.; Yu, C.-P. *Colloids Surf. A* **2014**, *444*, 226.
21. Jin, H.; Liu, X.; Gui, R.; Wang, Z. *Colloids Surf. B* **2015**, *128*, 498.
22. Kaiser, N.; Kimpfler, A.; Massing, U.; Burger, A. M.; Fiebig, H. H.; Brandl, M.; Schubert, R. *Int. J. Pharm.* **2003**, *256*, 123.
23. Varaprasad, K.; Vimala, K.; Ravindra, S.; Reddy, N. N.; Reddy, G. S. M.; Raju, K. M. *J. Polym. Environ.* **2012**, *20*, 573.
24. Jayaramudu, T.; Raghavendra, G. M.; Varaprasad, K.; Sadiku, R.; Raju, K. M. *Carbohydr. Polym.* **2013**, *92*, 2193.
25. Yadav, M.; Mun, S.; Hyun, J.; Kim, J. *Int. J. Biol. Macromol.* **2015**, *74*, 142.
26. Reddy, L. H.; Arias, J. L.; Nicolas, J.; Couvreur, P. *Chem. Rev.* **2012**, *112*, 5818.
27. Garcia, J.; Hsieh, M.-F.; Doma, B.; Peruelo, D.; Chen, I.-H.; Lee, H.-M. *Polymers* **2013**, *6*, 39.
28. Liang, J.; Cao, L.; Zhang, L.; Wan, X.-C. *Food Sci. Biotechnol.* **2014**, *23*, 569.
29. Zhu, B.; Li, J.; He, Y.; Yoshie, N.; Inoue, Y. *Macromol. Biosci.* **2003**, *3*, 684.
30. Shen, X.; Wang, Q.; Chen, W.; Pang, Y. *Appl. Surf. Sci.* **2014**, *317*, 1028.
31. Cui, Z.-M.; Jiang, L.-Y.; Song, W.-G.; Guo, Y.-G. *Chem. Mater.* **2009**, *21*, 1162.
32. Yu, B. Y.; Kwak, S.-Y. *J. Mater. Chem.* **2010**, *20*, 8320.
33. Orolínová, Z.; Mockovčiaková, A.; Zeleňák, V.; Myndyk, M. *J. Alloys Compd.* **2012**, *511*, 63.
34. Feltin, N.; Pileni, M. *Langmuir* **1997**, *13*, 3927.
35. Shan, Z.; Yang, W.-S.; Zhang, X.; Huang, Q.-M.; Ye, H. *J. Braz. Chem. Soc.* **2007**, *18*, 1329.
36. Bajpai, A.; Gupta, R. *Polym. Compos.* **2010**, *31*, 245.
37. Ghadban, A.; Ahmed, A. S.; Ping, Y.; Ramos, R.; Arfin, N.; Cantaert, B.; Ramanujan, R. V.; Miserez, A. *Chem. Commun.* **2016**, *52*, 697.
38. Weng, X.; Huang, L.; Chen, Z.; Megharaj, M.; Naidu, R. *Ind. Crops Prod.* **2013**, *51*, 342.
39. Jayaramudu, T.; Raghavendra, G. M.; Varaprasad, K.; Sadiku, R.; Ramam, K.; Raju, K. M. *Carbohydr. Polym.* **2013**, *95*, 188.
40. Nagireddy, N.; Yallapu, M.; Kokkarachedu, V.; Sakey, R.; Kanikireddy, V.; Pattayil Alias, J.; Konduru, M. J. *Polym. Res.* **2011**, *18*, 2285.
41. van Berkum, S.; Dee, J. T.; Philipse, A. P.; Erné, B. H. *Int. J. Mol. Sci.* **2013**, *14*, 10162.
42. Li, F.; Sun, J.; Zhu, H.; Wen, X.; Lin, C.; Shi, D. *Colloids Surf. B* **2011**, *88*, 58.

43. Varaprasad, K.; Reddy, N. N.; Ravindra, S.; Vimala, K.; Raju, K. M. *Int. J. Polym. Mater.* **2011**, *60*, 490.

44. Giani, G.; Fedi, S.; Barbucci, R. *Polymers* **2012**, *4*, 1157.

45. Zhao, W.; Odelius, K.; Edlund, U.; Zhao, C.; Albertsson, A.-C. *Biomacromolecules* **2015**, *16*, 2522.

46. Dobson, J. *Drug Dev. Res.* **2006**, *67*, 55.

47. Arruebo, M.; Fernández-Pacheco, R.; Ibarra, M. R.; Santamaría, J. *Nano Today* **2007**, *2*, 22.

48. Liu, T.-Y.; Hu, S.-H.; Liu, K.-H.; Liu, D.-M.; Chen, S.-Y. *J. Controlled Release* **2008**, *126*, 228.

49. Ekici, S.; Saraydin, D. *Polym. Int.* **2007**, *56*, 1371.

50. Ritger, P.; Peppas, N. *J. Controlled Release* **1987**, *19*, 37.